



Published in final edited form as:

Cell Rep. 2025 March 25; 44(3): 115409. doi:10.1016/j.celrep.2025.115409.

Microglia mediate the early-life programming of adult glucose control

Martin Valdearcos^{1,6,*}, Emily R. McGrath¹, Stephen M. Brown Mayfield¹, Melissa G. Jacuinde¹, Andrew Folick^{1,2}, Rachel T. Cheang¹, Ruoyu Li¹, Tomas P. Bachor¹, Rachel N. Lippert^{3,4,5}, Allison W. Xu¹, Suneil K. Koliwad^{1,2,6,7,*}

¹Diabetes Center, University of California, San Francisco, San Francisco, CA, USA

²Division of Endocrinology and Metabolism, Department of Medicine, University of California, San Francisco, San Francisco, CA, USA

³German Institute of Human Nutrition Potsdam Rehbrücke, Potsdam, Germany

⁴German Center for Diabetes Research, Neuherberg, Germany

⁵Max Planck Institute for Metabolism Research, Cologne, Germany

SUMMARY

Glucose homeostasis is, in part, nutritionally programmed during early neonatal life, a critical window for synapse formation between hypothalamic glucoregulatory centers. Although microglia prune synapses throughout the brain, their role in refining hypothalamic glucoregulatory circuits remains unclear. Here, we show that the phagocytic activity of microglia in the mediobasal hypothalamus (MBH) is induced following birth, regresses upon weaning from maternal milk, and is exacerbated by feeding dams a high-fat diet while lactating. In addition to actively engulfing synapses, microglia are critical for refining perineuronal nets (PNNs) within the neonatal MBH. Remarkably, transiently depleting microglia before weaning (postnatal day [P]6–16) but not afterward (P21–31) induces glucose intolerance in adulthood due to impaired insulin responsiveness, which we link to PNN overabundance and reduced synaptic connectivity between hypothalamic glucoregulatory neurons and the pancreatic β cell compartment. Thus, microglia facilitate early-life synaptic plasticity in the MBH, including PNN refinement, to program hypothalamic circuits regulating adult glucose homeostasis.

This is an open access article under the CC BY-NC license (<http://creativecommons.org/licenses/by-nc/4.0/>).

*Correspondence: martin.valdearcos@ucsf.edu (M.V.), suneil.koliwad@ucsf.edu (S.K.K.).

⁶These authors contributed equally

⁷Lead contact

AUTHOR CONTRIBUTIONS

Conceptualization, S.K.K. and M.V.; methodology, M.V., A.F., A.W.X., T.P.B., and R.N.L.; validation, M.V., E.R.M., S.M.B.M., M.G.J., R.T.C., and R.L.; formal analysis, M.V., A.F., E.R.M., M.G.J., T.P.B., and S.M.B.M.; investigation, M.V. and A.F.; resources, S.K.K., M.V., A.W.X., and R.N.L.; writing – original draft, M.V. and S.K.K.; writing – review & editing, S.K.K. and M.V.; visualization, M.V., E.R.M., T.P.B., S.M.B.M., S.K.K., and A.F.; supervision, S.K.K. and M.V.; project administration, S.K.K. and M.V.; funding acquisition, S.K.K. and M.V.

DECLARATION OF INTERESTS

The authors declare no competing interests.

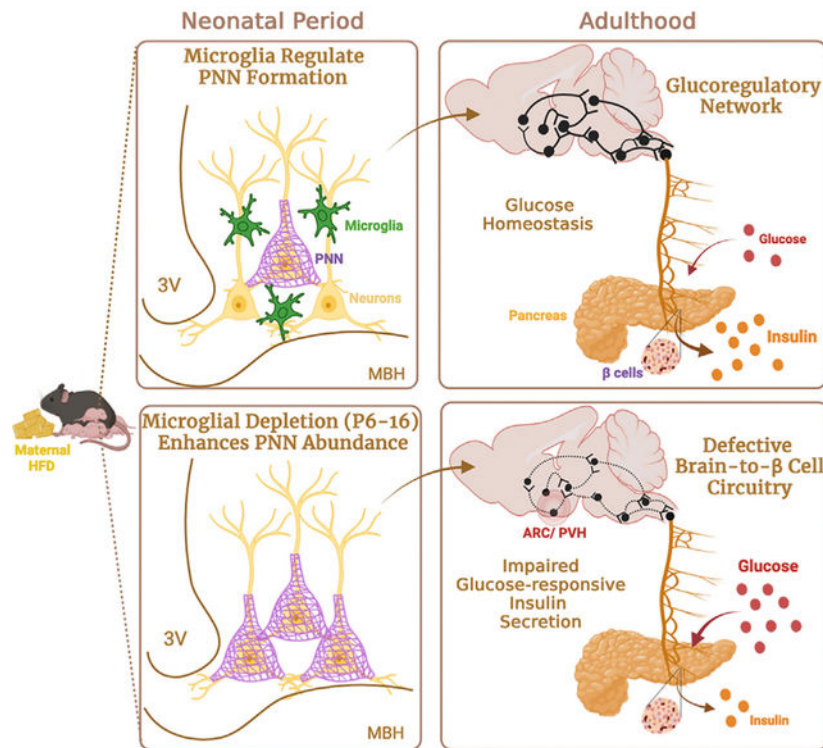
SUPPLEMENTAL INFORMATION

Supplemental information can be found online at <https://doi.org/10.1016/j.celrep.2025.115409>.

In brief

Valdearcos et al. show that microglia shape the hypothalamic perineuronal network during early postnatal life, ensuring that hypothalamic neurons projecting to the pancreatic β cell compartment during this time are maintained into adulthood. Depleting microglia in this critical period leaves mice incapable of secreting sufficient insulin when glucose challenged as adults.

Graphical Abstract



INTRODUCTION

The brain is increasingly recognized as a critical regulator of systemic glucose homeostasis,¹ and the intricate circuits involved in this regulation are beginning to be determined. These circuits integrate glucose sensory signaling with multiple effector mechanisms impinging on peripheral tissues controlling blood glucose. For instance, chemogenetically activating Agouti-related protein (AgRP) neurons in adult rodents acutely reduces systemic insulin sensitivity.² Specific glucose-sensing neurons in the hypothalamus also govern the release of insulin and glucagon from the pancreas through the autonomic nervous system,³ and disrupting these brain-to-islet circuits promotes manifestations of diabetes.^{4,5} Indeed, recent work has identified specific hypothalamic neurons that synaptically couple to the efferent autonomic fibers that supply pancreatic islets.⁶ This includes a recently uncovered brain-to- β cell trans-neural circuit regulating insulin secretion involving specific oxytocin neurons in the paraventricular nucleus of the hypothalamus (PVH) that receive input from AgRP neurons comprising the melanocortin system located in the arcuate nucleus (ARC) of the mediobasal hypothalamus (MBH).⁷

Circumstances occurring during early neonatal life are important in determining one's risk of developing diseases, such as type 2 diabetes, in adulthood.^{8,9} The hypothalamus is immature at birth and develops postnatally through the continuous projection of neuronal axons in the MBH that synapse onto specific targets to establish the melanocortin system. In rodents, for example, AgRP neurons develop axonal projections mainly during the second week of postnatal life,¹⁰ sending inputs to the PVH between postnatal day (P)8 and P10.¹¹ Proopiomelanocortin (POMC) neuronal projections display a similar temporal pattern.¹² The anatomical and temporal precision of the developmental connections that MBH neurons make with those in other brain regions are programmed by specific peripheral factors. For example, leptin, a hormone whose levels surge between P8 and P12 in mice, is essential for the developmental wiring of hypothalamic circuits¹³; treating leptin-deficient (ob/ob) mice with exogenous leptin until P28 restores neuronal projections that otherwise fail to form, whereas doing so after P28 is relatively ineffective by comparison.^{14,15}

Nutritional factors also influence CNS control of metabolic function. In particular, obese mothers and those consuming high-calorie diets when their offspring are still neonates increase the risk for an array of metabolic diseases when those offspring reach adulthood,¹⁶ a process termed “nutritional metabolic programming.” Similarly, rodents born to obese dams fed a high-fat diet (HFD) during gestation and/or lactation become progressively overweight, hyperphagic, and glucose intolerant as they grow into adults,^{16,17} metabolic alterations that are associated with disrupted development of AgRP and POMC projections to the PVH. Even when confined to the lactating period, maternal HFD consumption alters the development of hypothalamic neuronal circuits, causing obesity and hyperglycemia in the offspring.¹⁸ However, the hypothalamic sensors responsible for detecting hormonal, nutritional, and other metabolic signals during this critical window of susceptibility remain elusive. Similarly, the cellular mechanisms underlying how maternal malnutrition abnormally programs glucoregulatory MBH circuits are poorly understood.

We recently used both genetic deletion of key nuclear factor κ B (NF- κ B) regulators and chemogenetic strategies to show that altering microglial inflammatory responsiveness has a near-immediate effect on systemic glucose homeostasis.¹⁹ Specifically, activating microglia improved glucose tolerance in mice fed an HFD, an impact we linked to the regulation of hypothalamic glucose-sensing neurons in a manner independent of their previously identified role in regulating energy balance.¹⁹ However, the role that microglia may play in the early-life programming of CNS glucoregulatory circuits has not yet been studied.

Neuronal circuit development entails the formation, maturation, and stabilization of synapses, which consist of presynaptic and postsynaptic elements, the surrounding extracellular matrix (ECM), and glia, including microglia. The peptide hormone amylin, which influences neurogenesis, axonal fiber outgrowth, and leptin signaling in the hypothalamus,^{20–22} also enables the birth of microglia in the hypothalamic arcuate nucleus (ARC),²³ suggesting that the emergence of hypothalamic microglia is co-regulated along with hypothalamic circuit development during embryogenesis and early postnatal life. Moreover, using the colony-stimulating factor 1 receptor (CSF1R) inhibitor PLX5622 to deplete fetal microglia specifically during gestation reduces the number of postnatal POMC neurons in the MBH in association with accelerated weight gain starting at P5.²⁴

Microglia impact neuronal circuit organization through both synaptic pruning^{25–28} and ECM remodeling.^{29,30} Perineuronal nets (PNNs) are specialized reticular formations within the ECM of the CNS that scaffold neuronal synapses and guide synaptic plasticity, including during development.³¹ Microglia sculpt PNNs by releasing matrix metalloproteinases and other PNN-degrading proteases.³² Furthermore, recent work in mice shows that microglia remove PNNs in response to neuronally secreted interleukin (IL)-33; blocking this crosstalk impairs microglial phagocytosis and PNN engulfment, leading to impaired spine plasticity, reduced neonatal neuronal input integration, and impaired memory.³⁰ Intriguingly, postnatal PNN formation in the MBH coincides with the critical period during which AgRP neuronal circuits comprising the melanocortin system undergo maturation.³³ Indeed, it was recently shown that depleting microglia during early postnatal life is sufficient to increase PNN density and the overgrowth of AgRP neurons, suggesting that microglia impact the postnatal development of AgRP neurons by controlling PNN formation.³⁴

In this study, we show that early postnatal microglia help program adult glucose homeostasis in mice by shaping the connectivity between hypothalamic glucoregulatory neurons and the pancreatic β cell compartment, a process that involves a previously unrecognized role for microglia in guiding postnatal PNN refinement.

RESULTS

Microglia exhibit reactivity in the MBH of neonatal mice

We examined mice during the neonatal period when they rely on maternal milk for their nutritional needs. Mice matched for litter size were nursed by dams consuming either an HFD (Inotiv; TD.88137 Western diet, 42% from fat) or a standard low-fat chow diet (LFD; LabDiet 5053, 4.5% from fat) and underwent hypothalamic dissection at different time points either before weaning (P8 and P16, respectively) or 1 week after weaning (P28). Remarkably, we observed that both the number of microglia and the size of their cell bodies increased markedly from P8 to P16 specifically in the MBH, defined here as the hypothalamic region containing both the ARC and median eminence (ME) (Figures 1A–1C), but not in adjacent hypothalamic areas, such as the ventromedial nucleus of the hypothalamus (VMH), dorsomedial hypothalamic nucleus (DMH), or lateral hypothalamus (LH) (Figures S1A and S1B), or distant brain regions, such as the cerebral cortex (Figures S1C–S1E). Moreover, the response was transient, with a substantial regression seen by P28 after the mice had begun foraging for chow (Figures 1A–1C). Additionally, this transient MBH microglial response was accentuated when the dams consumed an HFD while lactating (Figures 1A–1C). Together, these findings prompted us to examine the extent to which these microglia regulate MBH circuit development.

Maternal HFD affects microglial synaptic engulfment and the formation of PNNs during the postnatal development of hypothalamic neuronal circuits

Microglia are crucial for postnatal synaptogenesis, working to eliminate weak or unnecessary synapses by selectively engulfing synaptic material for lysosomal degradation.^{35,36} Given that the synaptic connections forming the hypothalamic circuits controlling peripheral metabolism coincide both spatially and temporally with the microglial

reactivity we observed in the MBH of mice prior to weaning, we examined the involvement of these microglia in synapse elimination. To do so, we visualized the phagocytic activity of MBH microglia, along with synaptic material that they had internalized, using confocal microscopy and three-dimensional (3D) Imaris reconstructions (Figures 2A and 2B). Interestingly, both the overall phagocytic activity of MBH microglia, marked by CD68 positivity, and their synaptic engulfment, marked by intracellular postsynaptic density protein 95 (PSD-95), peaked at P16 and decreased after weaning (P28), indicating that these reactive microglia were engaged in synaptic refinement. Notably, these indicators of microglial phagocytosis and synaptic engulfment were further accentuated at P16 and exhibited less regression by P28 when the dams were fed an HFD (Figures 2C and 2D), suggesting that maternal HFD consumption both heightens and prolongs the demand on microglia to refine the synapses of MBH metabolic circuits. Taken together, these findings highlight the importance of microglia in mediating the interplay between maternal nutrition and synaptic plasticity within the MBH during early life.

Given that the maturation of AgRP neurons during the lactation period coincides with the formation of PNNs,³³ we also investigated the extent to which microglia remodel PNNs during this period. Consistent with previous studies,³³ we found that PNNs labeled with wisteria floribunda agglutinin (WFA) began appearing in the ARC between P8 and P16 and grew further by P28 (Figures 3A and 3B). Moreover, microglia in the ARC during this time were seen to engulf aggrecan, a core PNN protein, within CD68⁺ lysosomes (Figures 3C and 3D). As was observed for synaptic engulfment, PNN engulfment by MBH microglia during the neonatal period was increased when the dams were fed an HFD (Figures 3C and 3D). These data, together with our earlier findings, indicate that maternal diet dually influences synaptic and PNN engulfment by MBH microglia during a critical window when hypothalamic circuits that regulate peripheral metabolic homeostasis are developing.

Depleting microglia specifically during early life enforces a buildup of PNNs in the ARC and promotes glucose intolerance in adulthood

Based on these findings, we hypothesized that microglia may determine PNN density within the MBH during early postnatal life. To explore this, we used an inhibitor of CSF1R signaling (BLZ945, 200 mg/kg, ApexBio) to effectively and reversibly deplete CNS microglia in mice specifically before weaning from P6 to P16, with microglia fully repopulating the brains of mice within 5 days of stopping treatment (Figures 4A–4C). Doing so clearly increased PNN density in the MBH, highlighting the importance of microglia in sculpting these PNNs during early-life hypothalamic circuit development (Figures 4D and 4E).

We further hypothesized that the overabundance of PNNs in the MBH at the conclusion of the neonatal period resulting from this transient inhibition of microglial sculpting might alter the programming of peripheral metabolic control by the CNS. In testing this hypothesis, we first noted that prior to weaning, pups depleted of microglia gained less weight than control mice (Figure 5A), a finding resembling the impact of microglial depletion on the weight gain of HFD-fed adult mice in our prior studies.³⁷ Interestingly, upon discontinuing BLZ495 treatment and in association with the reconstitution of the microglial compartment,

the weights of the young mice rapidly normalized, with subsequent weight trajectories mirroring those of control mice that had retained their microglia throughout the study. However, glucose tolerance testing (GTT; 2 g/kg glucose, intraperitoneal [i.p.]) performed at 8 weeks of life revealed that mice depleted of microglia from P6 to P16 were remarkably glucose intolerant as adults vs. their control counterparts, despite both groups of mice having similar body weights when they were analyzed (Figures 5B and 5C). These data indicate that neonatal microglia are required to ensure normal systemic glucose tolerance in adulthood, an outcome that is not a function of differences in body weight gain.

To confirm the temporal importance of microglia in this aspect of metabolic programming, we examined a separate cohort of mice in which microglia were similarly depleted for a 10 day window but after weaning had already occurred (P21–P31). Doing so showed that unlike the clear impact of depleting microglia from P6 to P16, depleting microglia from P21 to P31 affected neither weight gain during the period of the depletion nor the glucose tolerance of the mice when they were assessed at 8 weeks of life (Figures 5D–5F). This lack of effectiveness was not a function of differences in the potency of CSF1 inhibition based on the age of the mice. Indeed, CSF1 inhibition depleted microglia in the brains of mice just as effectively from P21 to P31 as from P6 to P16 (Figure S2). These data also strongly suggest that our findings were not due to aberrant populations of microglia emerging in the brain following drug-induced depletion, as microglial repopulation occurred similarly following depletion both from P6 to P16 and from P21 to P31, but only depletion from P6 to P16 impacted the metabolic parameters we later analyzed.

To further convince ourselves that our findings were on target, we also treated mice from P6 to P16 with PLX73086, a different CSF1R inhibitor that does not penetrate the CNS.³⁸ Such treatment neither depleted microglia (Figures S3A–S3C) nor affected body weight (Figure S4D) or adult glucose tolerance (Figure S3E), indicating that our prior results were not due to the depletion of non-CNS myeloid populations. Taken together, our findings indicate that microglia are required during early neonatal life to ensure normal glucose tolerance in adulthood, supporting the concept that microglia play a role during early life in programming the capacity of the CNS to regulate glucose homeostasis in adulthood.

Given that low birth weight, including in humans, followed by catch-up growth during infancy can negatively impact glucose homeostasis and the risk for type 2 diabetes in adulthood,^{39,40} we also sought to ensure that our findings were not a function of the rapid weight normalization experienced by mice once neonatal microglial depletion was relieved. In examining this, we noted that neonatal microglial depletion impacted male and female mice differently. In both male and female mice, microglial depletion from P6 to P16 led to a slight reduction in weight gain during the period of depletion, followed by rapid body weight normalization upon discontinuation of CSF1R inhibition (Figure S4). By contrast, whereas depleting microglia from P6 to P16 caused adult glucose intolerance in male mice, this was not clearly seen in female mice (Figure S4). This sex-dependent difference, a topic for future studies, indicates that our findings in male mice are not simply a consequence of reduced neonatal weight gain followed by catch-up growth, as this phenomenon occurred in female mice as well. Additionally, although early-life microglial depletion impacted neonatal weight gain, it did not affect linear growth, an important detail given that small-for-

gestational-age babies who later exhibit impaired glucose metabolism usually have both reduced weight and length at birth.

Intriguingly, the impact of eliminating neonatal microglia on adult glucose intolerance was clearly evident when evaluating mice that had been nursed by dams consuming an HFD while lactating but was not as obvious when examining mice that had been nursed by dams fed a fat-sparing low-fat diet (Figure S5). This finding is concordant with our assessments of microglial number and phagocytic activity in the MBH, both of which were greatly increased during neonatal life by maternal consumption of an HFD, and suggests that maternally derived nutritional components, potentially including fats, may be important in driving microglia to engage in the developmental programming of metabolic circuits within the hypothalamus.

Microglia act during early life to ensure normal adult glucose-responsive pancreatic insulin secretion

Next, we sought to identify the determinant of systemic glucose homeostasis that is programmed by early-life microglia. We first noted that although depleting microglia (P6–P16) worsened adult glucose tolerance, it did not affect insulin tolerance (insulin tolerance test [ITT], 0.75 units per body weight: i.p.) (Figures 5G and 5H) or pyruvate tolerance (pyruvate tolerance test [PTT]) (Figures 5I and 5J), suggesting that our findings were not due to either impaired systemic insulin sensitivity or excessive hepatic glucose production. By contrast, mice lacking microglia from P6 to P16 had lower plasma insulin levels throughout GTTs performed at 8 weeks of life than controls, suggesting the possibility of reduced glucose-responsive pancreatic insulin secretion (Figures 6A and 6B). We explored this possibility by examining both the β cell mass and glucose responsiveness of pancreatic islets from pancreata isolated at 8 weeks of life from control mice vs. those having undergone microglial depletion from P6 to P16. We found that despite a clear loss of systemic glucose tolerance, the pancreatic islets of adult mice having undergone microglial depletion during early neonatal life both had a similar β cell mass (Figure 6C) and displayed similar glucose-stimulated insulin secretion (GSIS) dynamics (Figures 6D–6H) to those of control mice. Together, these findings suggest that if early-life microglia program the ability of the CNS to regulate adult pancreatic glucose responsiveness, they do not do so by impacting either β cell development or functional maturation per se. This conclusion and work indicating that autonomic control of glucose homeostasis is programmed during early life by maternal nutritional factors^{41,42} led us to explore instead the likelihood that microglia program the autonomic connectivity between the hypothalamus and the pancreatic β cell compartment.

Early-life microglia program the autonomic connectivity between the β cell compartment and the hypothalamus, including known glucoregulatory neuronal populations

With this question in mind, we developed a strategy to fluorescently trace the synaptic connectivity between the pancreatic β cell compartment and hypothalamic neurons, which are joined by autonomic fibers that communicate with key hypothalamic glucoregulatory centers.^{6,7} Using a minimally invasive surgical approach as previously described,²¹ we injected a new-generation pseudorabies virus (PRV-Ba2001) expressing a Cre-inducible GFP

reporter and the thymidine kinase enzyme (108 plaque-forming units [PFUs]/mL) into the pancreatic head, body, and tail regions of mouse insulin gene (*InsI*) promoter (MIP)-Cre^{ERT} mice, which express Cre specifically in β cells (Figures 7A and 7B). Upon subsequent tamoxifen treatment, this model enabled us to trace GFP fluorescence from the β cell compartment through neurons, including those comprising the autonomic nervous system, across multiple ascending synapses, and into specific hypothalamic nuclei, including the ARC and PVH, specifically in MIP-Cre^{ERT} mice but not Cre-negative littermates (Figure S6). Using this approach, we observed that transiently eliminating microglia in neonatal mice from P6 to P16 was remarkably sufficient to reduce the number of neurons within the ARC and the PVH that were specifically connected polysynaptically to the β cell compartment (GFP⁺) at 8 weeks of age (Figures 7C–7G). In exploring the identity of these β cell-connected hypothalamic neuronal populations, we found that 54% of these GFP⁺ cells were AgRP neurons residing in the ARC (Figure 7D), a population known to be crucial for CNS glucose regulation and that is already implicated in the impairment of adult glucose homeostasis induced during early life by maternal HFD consumption.¹⁸ Our data indicate that during the early neonatal period, microglia help program the ability of the CNS to properly potentiate glucose-responsive pancreatic insulin secretion in adulthood by determining the connectivity of hypothalamic neurons, including those involved in glucose sensing, with the pancreatic β cell compartment.

DISCUSSION

In this study, we show that in mice, microglia are reactive within the MBH during early neonatal life, working to prune synapses and sculpt PNNs in this brain region. Building on this, we reveal a previously unrecognized role for microglia during the early neonatal period, when mammals rely on maternal milk, in programming the synaptic connectivity of hypothalamic neurons with the pancreatic β cell compartment. Moreover, our work implicates this process as a determinant of the normal adult capacity to elevate insulin levels in response to rising systemic glucose concentrations.

Hypothalamic microglia as physiologically adaptive cells

Hypothalamic microglial reactivity was initially described in obese mice and humans over a decade ago.^{43,44} At the time, such reactivity was interpreted as a detrimental response to diet-induced hypothalamic injury, likely stemming from the classical observation that innate immune cells accumulate at sites of injury or infection and the finding that lipid accumulation, including long-chain saturated fats, can drive a pro-inflammatory reaction in tissue myeloid cells.^{45,46} Our understanding has significantly evolved from these early studies, with an increasing recognition of the ability of microglia to influence hypothalamic function in both physiologic and pathologic states. For instance, we recently demonstrated that inducing hypothalamic microglial inflammatory signaling in either lean or obese adult mice rapidly and unexpectedly benefits glycemic control by enhancing glucose disposal through a melanocortin-dependent pathway regulating pancreatic insulin secretion.¹⁹ The present study indicates that microglia are not only involved in acutely modulating CNS control over systemic glucose homeostasis during adult life but that they also help to shape the formation of synaptic connections during early life that enable the capacity for such

afferent control well after weaning. In this way, our work bolsters the emerging notion that microglia are assistive, rather than injurious, cells within the context of the developing hypothalamus, a concept that has implications not only for the early-life period but for our interpretation of the role of microglia within the adult hypothalamus as well.

Microglia shape synapses and PNNs in the developing MBH

Microglia are increasingly recognized as critical for regulating neuronal survival, for example, through the release of neurotrophic factors^{47,48} and for establishing neural wiring patterns during early postnatal brain development.^{47,48} In establishing such wiring, microglia guide the postnatal maturation and refinement of synaptic networks. Our data here indicate that at ~P16, reactive microglia marked by enlarged cell bodies and heightened phagocytic activity actively engage in synaptic engulfment in the MBH, as measured by internalized PSD-95⁺ puncta, coinciding with the development of AgRP and POMC axonal projections.¹¹ Certain “eat me” signals, such as complement cascade components C1q and C3, have been shown to promote inappropriate and/or extraneous synapse engulfment by microglia through C3 receptor signaling.^{49,50} By contrast, “don’t eat me” signals, such as CD47, serve to negatively regulate synaptic pruning and thus avoid excess synapse elimination.⁵¹ Further studies are needed to determine the signals by which maternal diet influences microglial phagocytic activity during the development of hypothalamic neural circuits.

Unlike in the MBH, we did not observe reactive microglia in the cerebral cortices of neonatal mice even in the context of maternal HFD feeding. Despite this, we cannot conclude that the induction of neonatal microglial reactivity in response to maternal HFD consumption is exclusive to the MBH. Indeed, exposure to a hypercaloric environment during the early postnatal developmental period can have lasting and potentially deleterious effects on microglial number and function across multiple brain regions in age- and sex-specific ways.⁵² For example, neonatal overnutrition was reported to influence hippocampal microglial in both male and female rats.⁵³ Furthermore, neonatal overfeeding increased hippocampal susceptibility to microgliosis following a subsequent immune challenge, for example, i.p. lipopolysaccharide (LPS) injection.⁵³

Microglia also modify the extent to which the ECM allows synaptic projections to connect with their desired targets. PNNs are unique reticular ECM formations that encapsulate the soma and dendrites of certain neurons in the brain, such as fast-spiking, parvalbumin-positive inhibitory neurons. PNN formation occurs during critical periods of developmental plasticity, and microglia are integral in remodeling PNNs in both healthy and diseased states,²⁹ regulating the balance between their formation and degradation via both direct and indirect enzymatic/phagocytic processes.^{54–56} Notably, PNN deficiency in the ARC of postnatal ob/ob mice can be restored by leptin administration during postnatal development,³³ and recent work showed that chemically disrupting PNNs in the MBH attenuates the glucose-lowering effects of centrally acting fibroblast growth factor 1 (FGF1) in obese Zucker diabetic fatty (ZDF) rats,⁵⁷ indicating a potential role of PNNs in regulating glucose homeostasis. A recent study demonstrated that an obesogenic diet induced an abnormal accumulation of PNNs in the ARC of adult mice, creating a barrier to

insulin signaling and leading to increased food intake and weight gain.⁵⁸ This phenomenon, termed “neurofibrosis,” arises from a reduction in levels of ECM-degrading enzymes and an increase in enzymatic inhibition ostensibly driven by hypothalamic microgliosis.⁵⁸ Pharmacological disassembly of PNNs in obese mice reversed metabolic dysfunction, underscoring neurofibrosis as a key mediator of diet-induced metabolic disease.⁵⁸ Here, we show that postnatal microglial depletion enforces an accumulation of PNNs in the MBH, findings that align with a recent study suggesting that microglia influence AgRP postnatal development by remodeling PNN-dependent synaptic plasticity.³⁴ This is important given that PNNs enmesh AgRP neurons in the MBH and because their formation coincides with the critical period during which early postnatal AgRP neuronal maturation is influenced by leptin.³³ Indeed, depleting microglia in mice during the second week after birth increases leptin sensitivity and causes an abnormal rise in AgRP neuronal number and fiber density in the ARC.³⁴ However, further research is needed to establish a causal relationship between microglial regulation of neonatal PNN abundance and leptin sensitivity.

A brain-to- β cell circuit developmentally programmed by microglia

Synaptic tracing studies and chemogenetic manipulations targeting distinct hypothalamic neuronal subpopulations have provided new insights into how the brain regulates the β cell insulin secretory response to hypoglycemia.⁷ For example, a subpopulation of oxytocin neurons in the PVN was recently revealed to comprise a circuit activated by glucoprivation that suppresses insulin secretion by pancreatic β cells via the sympathetic autonomic nervous system. Another recent study by Bruning and colleagues used optogenetic and chemogenetic approaches to show that AgRP neuronal activation induces hepatic autophagy as part of a hypothalamic-liver axis that is metabolically adaptative during nutrient deprivation.⁵⁹ Here, we map brain-to- β cell synaptic connections as a means to reveal that early postnatal microglia are required for the functional development of efferent glucoregulatory circuits emanating from the MBH that are connected to the β cell compartment. Although our analysis identifies projections from AgRP neurons in both the ARC and PVN as being among those shaped by microglia during early life, future studies will need to focus on additional neuronal subsets across a broader array of brain regions. In addition, we do not know the extent to which microglia are also required for the programming synaptic connectivity between the brain and other peripheral metabolic organs, such as liver, that regulate glucose homeostasis.

The alterations in CNS programming that lead to increases in the risk for cardiometabolic disease later in life display sex-dependent skewing.⁶⁰ For example, data from mice suggest that female pups are more susceptible to developing impaired glucose tolerance as adults in response to programming during gestation.⁶¹ However, the mechanisms underlying these and other sex-based differences are not understood. In our study, both male and female mice displayed a similar modest body weight reduction during microglial depletion, followed by rapid catch-up growth after drug withdrawal and consequent microglial repopulation of the brain. However, such transient microglial depletion, when performed prior to weaning, impacted adult glucose homeostasis only in the male mice we examined, despite the fact that our strategy to deplete microglia was equally effective in both sexes. With this in mind, we note that there is a growing appreciation of sex differences in microglial differentiation

within the brain.⁶² Indeed, there are sex differences in microglial gene expression and phagocytic activity during brain development.^{63,64} Microglia also contribute to the sexual dimorphism of the developing brain. For instance, they are essential for the masculinization of the hypothalamic preoptic area, a region critical for regulating male sexual behaviors.⁶⁵ Furthermore, transient microglial depletion during the early postnatal period leads to defects in male-specific sex behaviors that last into adulthood.⁶⁶ Additional studies are needed to understand the sex-specific ways by which microglia shape glucoregulatory synapses within the hypothalamus during early life.

In summary, we show that prior to weaning, microglia shape PNNs within the MBH and that depleting microglia, particularly in the context of a maternal HFD, notably increases PNN density during this critical early-life period. PNN overabundance in the MBH due to microglial depletion, in turn, reduces the connectivity between key hypothalamic glucoregulatory neurons and pancreatic β cells, the consequence of which is impaired glucose-responsive insulin secretion and relative glucose intolerance in adulthood.

Limitations of the study

We acknowledge some limitations of the work presented here. First, our studies alone do not prove that the reduced brain-to- β cell synaptic connectivity in adult mice following neonatal microglial depletion is the specific cause of the impaired insulin secretion and adult glucose tolerance we observed. Indeed, this is exceptionally difficult to determine without a temporal gain-of-function approach to independently restore synaptic connectivity despite early-life microglial depletion. Current tools and techniques preclude such a definitive study, although future work should seek to profile a wider array of potential brain glucoregulatory circuits modulated by microglia during the neonatal period. Additionally, our studies do not prove that diminished brain-to- β cell synaptic connectivity is a direct consequence of altered PNN density within the MBH. Although studies have effectively used enzymatic approaches to diminish PNNs in anatomically defined regions of the brain in adult mice,⁵⁷ such approaches are simply not yet feasible in early neonatal mice. Still, the literature has strongly implicated PNNs in modulating hypothalamic neuronal projections, including those regulating blood glucose,⁵⁷ and so our conclusion is, in our view, logical.

RESOURCE AVAILABILITY

Lead contact: Requests for further information, resources, and reagents should be directed to and will be fulfilled by the lead contact, Suneil K. Koliwad (suneil.koliwad@ucsf.edu).

Materials availability: This study did not generate new unique reagents.

Data and code availability

- Any data reported in this paper will be shared by the lead contact upon request.
- This paper does not report original code.
- Any additional information needed to reanalyze the data reported in this paper is available from the lead contact upon request.

STAR★METHODS

EXPERIMENTAL MODEL AND STUDY PARTICIPANT DETAILS

Animal husbandry: The studies presented here involved mice on the C57BL/6J background, with backcrossing done to avoid genetic drift, and all procedures were performed in accordance with NIH Guidelines for Care and Use of Animals and were approved by the Institutional Animal Care and Use Committees at the University of California San Francisco. Unless otherwise specified, all mice were group-housed and age-matched with *ad libitum* access to water and a specified diet in a pathogen- and temperature-controlled room with a 12:12h light: dark cycle. Mice were fed either a standard low-fat CD (LabDiet 5053) or an HFD in which 42% of total kcals were from fat (Inotiv; TD.88137 Western Diet). Whenever possible, littermates of the same sex were randomly assigned to experimental groups. Anesthesia was by isoflurane, 100 mg/kg ketamine, and 10 mg/kg xylazine or Avertin (terminal procedures).

Mice: Studies involving PRV-Ba2001 polysynaptic tracing used MIP-CreERT (JAX, 024709) adult male mice (10–14 weeks of age) in which nuclear Cre expression is restricted to pancreatic β -cells when induced by tamoxifen treatment as described.⁶ The appropriate progeny resulting from crosses of these mice and corresponding controls received three 5 mg doses of tamoxifen (MP Biomedicals, 10540–29-1) dissolved in 200 μ L warm purified corn oil by enteric gavage in order to induce Cre expression. All other studies used WT C57BL/6J mice. Microglia were depleted in separate cohorts of both male and female mice using small molecule inhibitors of CSF1R. For microglial depletion post-weaning, mice were administered the CSF1R inhibitor PLX5622 (Plexxikon) formulated in a low-fat CD (AIN-76A, Research Diets) at a dose of 1.2 g/kg. For microglial depletion prior to weaning, neonatal mice were injected subcutaneously with BLZ945 (APExBIO, B4899, 200 mg/kg, every other day), another CSF1R inhibitor, dissolved in 20% Captisol (Cydex, RC0C7100, beta-cyclodextrin sulfobutyl ethers, sodium salts) as described previously.⁶

METHOD DETAILS

PRV retrograde polysynaptic neuronal tracing: PRV-Ba2001 was acquired by PNI (Princeton Neuroscience Institute) Viral Vector Core facility. A total of 10 μ L of PRV-Ba2001 vector (10^8 plaque-forming units [pfu]/mL) was injected in three separate sites in the head, body, and tail regions of a mouse pancreas by intra-abdominal surgery as described previously.⁶ Animals were sacrificed 120h post-surgery and brains were harvested, fixed in 4% (v/v) paraformaldehyde, and embedded in M-1 Embedding Matrix (Eppredia 1310).

Body composition analysis in awake, conscious mice: Body composition analyses including quantification of fat mass and lean mass, were performed at the NIDDK-funded Nutrition Obesity Research Center (NORC) metabolic core at UCSF, using EchoMRI in awake, conscious mice (EchoMRI-3in1, Echo Medical Systems, Houston, TX.).

In vivo assessments of glucose homeostasis: Glucose tolerance tests (GTT) were performed as described previously. Briefly, animals were fasted for 6h (09:00–15:00) prior to glucose administration (D-(+)-glucose, 20% solution, 2 g/kg, i.p: Teknova). Glucose was

measured in tail blood by a hand-held glucometer. Total glucose area-under-curve (AUC) and excursion were measured by the trapezoid rule. Glucose-stimulated insulin secretion was performed as in the GTT with minor modifications. Glucose (2 g/kg/lean mass i.p.) was administered with collection of tail blood at 0, 5, 15, or 30 min for insulin tolerance tests (ITT) were performed as described previously. Briefly, animals were fasted for 4h (09:00–13:00) and administered insulin (Novolin, 0.75 units per body weight: i.p.). Glucose was measured in tail blood by glucometer. Pyruvate tolerance tests (PTT) were performed as described previously. Briefly, animals were fasted for 6h (09:00–15:00) and administered pyruvate (2 g/kg, i.p.; Sigma). Glucose was measured in tail blood by glucometer.

Hypothalamic image analyses: WFA quantification: Quantification of the PNN marker WFA was performed on confocal images at 63x magnification (10µm stacks, 8 slices total, 1024 × 1024 resolution). A summative projection of slices in the WFA channel was created, and a region of interest was drawn based on the maximal DAPI projection and applied to the projection from the WFA channel. Total WFA area was calculated based on mean gray value/MFI as measured using FIJI image processing package (ImageJ, “batteries included”).

CD68 quantification: The intracellular lysosomal marker CD68 was quantified from confocal images (1024 × 1024, 200 Hz) of MBH sections. Cell surface CD68 staining positivity was then quantified based on 3D reconstructions performed on Imaris at 0.1µm surface detail with 2µm background subtraction and thresholding to an arbitrary value of 24.3 surfaces recorded per image.

Aggrecan quantification: Quantification of the PNN marker Aggrecan was achieved via 3D Imaris reconstruction using a mask based on the CD68 signal and surface construction with the following specifications: 0.2 µm surface detail, 3µm background subtraction and thresholding to a value of 10.5 surfaces recorded per image.

Pancreatic islet isolation and *in vitro* assessment of insulin secretion: Islets were isolated by the Vanderbilt Islet and Pancreas Analysis (IPA) core by injecting 0.6 mg/mL collagenase P (Roche) into the pancreatic bile duct followed by a Histopaque-1077 (Sigma) fractionation and hand-picking. Isolated islets were cultured overnight in low glucose DMEM (Thermo, 11966–025) containing 1 g/L glucose and supplemented with 10% FBS (Atlanta Biologicals), 4.6 mM HEPES, 1% penicillin/streptomycin (Thermo), 1% non-essential amino acids (Sigma) in a sterile cell incubator at 37°C with 5% CO₂ infusion and 95% humidity. Glucose-stimulated insulin secretion (GSIS) was assessed by perfusion with the use of size-matched islets and normalized to islet equivalents as previously described.⁶⁷ Briefly, the GSIS protocol included three secretagogues, glucose (16.7 mmol/L), 3-isobutyl-1-methylxanthine (IBMX) (100 µmol/L), and KCL (20mmol/L), in sequence. Insulin in the culture medium was determined by ELISA.

Pancreas immunohistochemistry and morphometric analysis: Pancreata tissues were embedded in paraffin wax and sectioned to 6-µm thickness. Islet β- and α-cell areas were determined as described previously.⁶⁸ Briefly, pancreatic sections taken every 50 µm (*n* = 5 animals per condition) were scanned using a ScanScope CS scanner (Aperio Technologies, Vista, CA). Images from each experiment were processed with

ImageScope Software (Aperio Technologies, Vista, CA). Islet band α -cell areas were calculated as the ratio of the insulin-or glucagon-positive area to the total pancreas area (eosin stained). Primary anti-mouse antibodies were against Iba1 (1:500, rabbit polyclonal, Wako, and 1:500, goat polyclonal, Abcam), CD68 (1:500, rat, Biorad) PSD95 (1:500, rabbit polyclonal, Synaptic Systems) Wisteria floribunda lectin (WFA, 1:500, Biotinylated, Vector Laboratories), Aggrecan (1:500, rabbit polyclonal, Millipore) AgRP (1:500, goat, Neuromics), GFP (1:500, chicken, Aves Labs), insulin (1:250, guinea pig, Fitzgerald industries), glucagon (1:100, rabbit, Cell Signaling) and somatostatin (1:500, goat, Santa Cruz Biotechnology). Adequate AlexaFluor-conjugated secondary antibodies were used for immunofluorescence microscopy. Sections were mounted with DAPI Vectashield solution (Vector Laboratories, Inc.) to identify cell nuclei. Images were acquired with a confocal laser-scanning microscope (Leica TCS SP8). Islet size was then assessed using MetaMorph, version 7.7 (Universal Imaging).

Microglial cell counting and analysis of microglial phagocytic activity from histological brain sections: Anesthetized mice were perfused with saline and 4% paraformaldehyde in 100mM phosphate buffer, and their brains were dissected, postfixed in the same fixative overnight (4°C), and immersed in 30% sucrose. Hypothalamic tissues were then separated from other regions, embedded in optimal cutting temperature compound, immediately frozen on dry ice, and stored at -80°C. Next, 35- μ M-thick hypothalamic coronal sections were cut on a cryostat, blocked for 1 h with 5% BSA in PBS containing 0.1% Triton X-100, and incubated with primary antibodies overnight at 4°C. Iba1+ cells in hypothalamic sections were counted manually by visual inspection of anatomically matched within prespecified regions of interest, with an average taken from three sequential sections per mouse. Primary anti-mouse antibodies were against Iba1 (1:500, rabbit polyclonal, Wako, and 1:500, goat polyclonal, Abcam), CD68 (1:500, rat, Biorad) PSD95 (1:500, rabbit polyclonal, Synaptic Systems), Wisteria floribunda lectin (WFA, 1:500, Biotinylated, Vector Laboratories), Aggrecan (1:500, rabbit polyclonal, Millipore), AgRP (1:500, goat, Neuromics), and GFP (1:500, chicken, Aves Labs). AlexaFluor-conjugated secondary antibodies were used for immunofluorescence microscopy. Sections were mounted with DAPI Vectashield solution (Vector Laboratories, Inc.) to identify cell nuclei. Images were acquired with a confocal laser-scanning microscope (Leica TCS SP8). Microglial cell body size was determined by ImageJ software using a thresholding protocol (ImageJ) followed by densitometric quantification. WFA fluorescence intensity was similarly measured with ImageJ software from images captured using identical exposure times that also avoided saturating the pixel intensities. Imaris software 9.5.1 was used to create surface renderings of individual microglia cells labeled with Iba1, incomplete or poorly labeled cells were excluded from analyses. CD68, PSD95, and aggrecan content within the microglia surface were quantified. The volume of phagocytes and engulfed synapses was normalized to cell volume.

QUANTIFICATION AND STATISTICAL ANALYSIS

We analyzed all data using GraphPad Prism version 8.0 software (San Diego, CA). Data are presented as mean \pm SEM. Two groups were compared using an unpaired two-tail Student's t-test. One-way ANOVAs were used to analyze datasets with more than two

groups. Two-way ANOVAs were used to analyze datasets with two independent variables, followed by Bonferroni post-hoc adjustment. *p* values of less than 0.05 were considered significant.

Supplementary Material

Refer to Web version on PubMed Central for supplementary material.

ACKNOWLEDGMENTS

This work was supported by the Larry L. Hillblom Foundation (Start-Up grant to M.V.) and the NIDDK (R01 DK134782-01 to M.V. and R01 DK103175-02 to S.K.K.). Metabolic phenotyping was assisted by the NIDDK-sponsored Nutrition Obesity Research Center at UCSF (DK098722). Islet isolation and functional analysis were performed using the Islet and Pancreas Analysis (IPA) Core in the NIDDK-sponsored Vanderbilt Diabetes Research Center (DK20593). The authors would like to thank Dr. Jens Bruning (Cologne, Germany) for helpful technical advice and insights.

REFERENCES

1. Ruud J, Steculorum SM, and Brüning JC (2017). Neuronal control of peripheral insulin sensitivity and glucose metabolism. *Nat. Commun.* 8, 15259. 10.1038/ncomms15259. [PubMed: 28469281]
2. Steculorum SM, Ruud J, Karakasilioti I, Backes H, Engström Ruud L, Timper K, Hess ME, Tsaousidou E, Mauer J, Vogt MC, et al. (2016). Agrp neurons control systemic insulin sensitivity via myostatin expression in brown adipose tissue. *Cell* 165, 125–138. 10.1016/j.cell.2016.02.044. [PubMed: 27015310]
3. Faber CL, Deem JD, Campos CA, Taborsky GJ, and Morton GJ (2020). CNS control of the endocrine pancreas. *Diabetologia* 63, 2086–2094. 10.1007/s00125-020-05204-6. [PubMed: 32894319]
4. Carey M, Kehlenbrink S, and Hawkins M (2013). Evidence for central regulation of glucose metabolism. *J. Biol. Chem.* 288, 34981–34988. 10.1074/jbc.R113.506782. [PubMed: 24142701]
5. Yoon NA, and Diano S (2021). Hypothalamic glucose-sensing mechanisms. *Diabetologia* 64, 985–993. 10.1007/s00125-021-05395-6. [PubMed: 33544170]
6. Rosario W, Singh I, Wautlet A, Patterson C, Flak J, Becker TC, Ali A, Tamarina N, Philipson LH, Enquist LW, et al. (2016). The Brain-to-Pancreatic Islet Neuronal Map Reveals Differential Glucose Regulation From Distinct Hypothalamic Regions. *Diabetes* 65, 2711–2723. 10.2337/db15-0629. [PubMed: 27207534]
7. Papazoglou I, Lee J-H, Cui Z, Li C, Fulgenzi G, Bahn YJ, Staniszevska-Goraczniak HM, Piñol RA, Hogue IB, Enquist LW, et al. (2022). A distinct hypothalamus-to- β cell circuit modulates insulin secretion. *Cell Metab.* 34, 285–298.e7. 10.1016/j.cmet.2021.12.020. [PubMed: 35108515]
8. Li M, Sloboda DM, and Vickers MH (2011). Maternal obesity and developmental programming of metabolic disorders in offspring: evidence from animal models. *Exp. Diabetes Res.* 2011, 592408. 10.1155/2011/592408. [PubMed: 21969822]
9. Gaillard R, Felix JF, Duijts L, and Jaddoe VWV (2014). Childhood consequences of maternal obesity and excessive weight gain during pregnancy. *Acta Obstet. Gynecol. Scand.* 93, 1085–1089. 10.1111/aogs.12506. [PubMed: 25231923]
10. Grove KL, Allen S, Grayson BE, and Smith MS (2003). Postnatal development of the hypothalamic neuropeptide Y system. *Neuroscience* 116, 393–406. 10.1016/s0306-4522(02)00668-1. [PubMed: 12559095]
11. Bouret SG, Draper SJ, and Simerly RB (2004). Formation of projection pathways from the arcuate nucleus of the hypothalamus to hypothalamic regions implicated in the neural control of feeding behavior in mice. *J. Neurosci.* 24, 2797–2805. 10.1523/JNEUROSCI.5369-03.2004. [PubMed: 15028773]
12. Nilsson I, Johansen JE, Schalling M, Hökfelt T, and Fetisov SO (2005). Maturation of the hypothalamic arcuate agouti-related protein system during postnatal development in the

- mouse. *Brain Res. Dev. Brain Res.* 155, 147–154. 10.1016/j.devbrainres.2005.01.009. [PubMed: 15804403]
13. Ahima RS, Prabakaran D, and Flier JS (1998). Postnatal leptin surge and regulation of circadian rhythm of leptin by feeding. Implications for energy homeostasis and neuroendocrine function. *J. Clin. Invest.* 101, 1020–1027. 10.1172/JCI11176. [PubMed: 9486972]
 14. Bouret SG, Draper SJ, and Simerly RB (2004). Trophic action of leptin on hypothalamic neurons that regulate feeding. *Science* 304, 108–110. 10.1126/science.1095004. [PubMed: 15064420]
 15. Kamitakahara A, Bouyer K, Wang C-H, and Simerly R (2018). A critical period for the trophic actions of leptin on AgRP neurons in the arcuate nucleus of the hypothalamus. *J. Comp. Neurol.* 526, 133–145. 10.1002/cne.24327. [PubMed: 28891045]
 16. Chen H, Simar D, and Morris MJ (2009). Hypothalamic neuroendocrine circuitry is programmed by maternal obesity: interaction with postnatal nutritional environment. *PLoS One* 4, e6259. 10.1371/journal.pone.0006259. [PubMed: 19606226]
 17. Kirk SL, Samuelsson A-M, Argenton M, Dhonye H, Kalamatianos T, Poston L, Taylor PD, and Coen CW (2009). Maternal obesity induced by diet in rats permanently influences central processes regulating food intake in offspring. *PLoS One* 4, e5870. 10.1371/journal.pone.0005870. [PubMed: 19516909]
 18. Vogt MC, Paeger L, Hess S, Steculorum SM, Awazawa M, Hampel B, Neupert S, Nicholls HT, Mauer J, Hausen AC, et al. (2014). Neonatal insulin action impairs hypothalamic neurocircuit formation in response to maternal high-fat feeding. *Cell* 156, 495–509. 10.1016/j.cell.2014.01.008. [PubMed: 24462248]
 19. Douglass JD, Ness KM, Valdearcos M, Wyse-Jackson A, Dorfman MD, Frey JM, Fasnacht RD, Santiago OD, Niraula A, Banerjee J, et al. (2023). Obesity-associated microglial inflammatory activation paradoxically improves glucose tolerance. *Cell Metab.* 35, 1613–1629.e8. 10.1016/j.cmet.2023.07.008. [PubMed: 37572666]
 20. Abegg K, Hermann A, Boyle CN, Bouret SG, Lutz TA, and Riediger T (2017). Involvement of Amylin and Leptin in the Development of Projections from the Area Postrema to the Nucleus of the Solitary Tract. *Front. Endocrinol.* 8, 324. 10.3389/fendo.2017.00324.
 21. Liberini CG, Borner T, Boyle CN, and Lutz TA (2016). The satiating hormone amylin enhances neurogenesis in the area postrema of adult rats. *Mol. Metabol.* 5, 834–843. 10.1016/j.molmet.2016.06.015.
 22. Lutz TA, Coester B, Whiting L, Dunn-Meynell AA, Boyle CN, Bouret SG, Levin BE, and Le Foll C (2018). Amylin selectively signals onto POMC neurons in the arcuate nucleus of the hypothalamus. *Diabetes* 67, 805–817. 10.2337/db17-1347. [PubMed: 29467172]
 23. Lutz TA, and Le Foll C (2019). Endogenous amylin contributes to birth of microglial cells in arcuate nucleus of hypothalamus and area postrema during fetal development. *Am. J. Physiol. Regul. Integr. Comp. Physiol.* 316, R791–R801. 10.1152/ajpregu.00004.2019. [PubMed: 30943041]
 24. Rosin JM, Vora SR, and Kurrasch DM (2018). Depletion of embryonic microglia using the CSF1R inhibitor PLX5622 has adverse sex-specific effects on mice, including accelerated weight gain, hyperactivity and anxiolytic-like behaviour. *Brain Behav. Immun.* 73, 682–697. 10.1016/j.bbi.2018.07.023. [PubMed: 30056204]
 25. Thion MS, Ginhoux F, and Garel S (2018). Microglia and early brain development: An intimate journey. *Science* 362, 185–189. 10.1126/science.aat0474. [PubMed: 30309946]
 26. Bohlen CJ, Friedman BA, Dejanovic B, and Sheng M (2019). Microglia in brain development, homeostasis, and neurodegeneration. *Annu. Rev. Genet.* 53, 263–288. 10.1146/annurev-genet-112618-043515. [PubMed: 31518519]
 27. Neniskyte U, and Gross CT (2017). Errant gardeners: glial-cell-dependent synaptic pruning and neurodevelopmental disorders. *Nat. Rev. Neurosci.* 18, 658–670. 10.1038/nrn.2017.110. [PubMed: 28931944]
 28. Wilton DK, Dissing-Olesen L, and Stevens B (2019). Neuron-Glia Signaling in Synapse Elimination. *Annu. Rev. Neurosci.* 42, 107–127. 10.1146/annurev-neuro-070918-050306. [PubMed: 31283900]

29. Crapser JD, Arreola MA, Tsourmas KI, and Green KN (2021). Microglia as hackers of the matrix: sculpting synapses and the extracellular space. *Cell. Mol. Immunol.* 18, 2472–2488. 10.1038/s41423-021-00751-3. [PubMed: 34413489]
30. Nguyen PT, Dorman LC, Pan S, Vainchtein ID, Han RT, Nakao-Inoue H, Taloma SE, Barron JJ, Molofsky AB, Kheirbek MA, and Molofsky AV (2020). Microglial remodeling of the extracellular matrix promotes synapse plasticity. *Cell* 182, 388–403.e15. 10.1016/j.cell.2020.05.050. [PubMed: 32615087]
31. Reichelt AC, Hare DJ, Bussey TJ, and Saksida LM (2019). Perineuronal nets: plasticity, protection, and therapeutic potential. *Trends Neurosci.* 42, 458–470. 10.1016/j.tins.2019.04.003. [PubMed: 31174916]
32. Wen TH, Binder DK, Ethell IM, and Razak KA (2018). The perineuronal “safety” net? perineuronal net abnormalities in neurological disorders. *Front. Mol. Neurosci.* 11, 270. 10.3389/fnmol.2018.00270. [PubMed: 30123106]
33. Mirzadeh Z, Alonge KM, Cabrales E, Herranz-Pérez V, Scarlett JM, Brown JM, Hassouna R, Matsen ME, Nguyen HT, Garcia-Verdugo JM, et al. (2019). Perineuronal Net Formation during the Critical Period for Neuronal Maturation in the Hypothalamic Arcuate Nucleus. *Nat. Metab.* 1, 212–221. 10.1038/s42255-018-0029-0. [PubMed: 31245789]
34. Sun J, Wang X, Sun R, Xiao X, Wang Y, Peng Y, and Gao Y (2024). Microglia shape AgRP neuron postnatal development via regulating perineuronal net plasticity. *Mol. Psychiatr.* 29, 306–316. 10.1038/s41380-023-02326-2.
35. Schafer DP, Lehrman EK, Kautzman AG, Koyama R, Mardinly AR, Yamasaki R, Ransohoff RM, Greenberg ME, Barres BA, and Stevens B (2012). Microglia sculpt postnatal neural circuits in an activity and complement-dependent manner. *Neuron* 74, 691–705. 10.1016/j.neuron.2012.03.026. [PubMed: 22632727]
36. Weinhard L, di Bartolomei G, Bolasco G, Machado P, Schieber NL, Neniskyte U, Exiga M, Vadiute A, Raggioli A, Schertel A, et al. (2018). Microglia remodel synapses by presynaptic trogocytosis and spine head filopodia induction. *Nat. Commun.* 9, 1228. 10.1038/s41467-018-03566-5. [PubMed: 29581545]
37. Valdearcos M, Douglass JD, Robblee MM, Dorfman MD, Stifler DR, Bennett ML, Gerritse I, Fasnacht R, Barres BA, Thaler JP, and Koliwad SK (2017). Microglial inflammatory signaling orchestrates the hypothalamic immune response to dietary excess and mediates obesity susceptibility. *Cell Metab.* 26, 185–197.e3. 10.1016/j.cmet.2017.05.015. [PubMed: 28683286]
38. Bellver-Landete V, Bretheau F, Mailhot B, Vallières N, Lessard M, Janelle M-E, Vernoux N, Tremblay MÈ, Fuehrmann T, Shoichet MS, and Lacroix S (2019). Microglia are an essential component of the neuroprotective scar that forms after spinal cord injury. *Nat. Commun.* 10, 518. 10.1038/s41467-019-08446-0. [PubMed: 30705270]
39. Cianfarani S, Germani D, and Branca F (1999). Low birthweight and adult insulin resistance: the “catch-up growth” hypothesis. *Arch. Dis. Child. Fetal Neonatal Ed.* 81, F71–F73. 10.1136/fn.81.1.f71. [PubMed: 10375369]
40. Veening MA, Van Weissenbruch MM, and Delemarre-Van De Waal HA (2002). Glucose tolerance, insulin sensitivity, and insulin secretion in children born small for gestational age. *J. Clin. Endocrinol. Metab.* 87, 4657–4661. 10.1210/jc.2001-011940. [PubMed: 12364453]
41. Cottrell EC, and Ozanne SE (2008). Early life programming of obesity and metabolic disease. *Physiol. Behav.* 94, 17–28. 10.1016/j.physbeh.2007.11.017. [PubMed: 18155097]
42. Bouret SG (2012). Nutritional programming of hypothalamic development: critical periods and windows of opportunity. *Int. J. Obes. Suppl.* 2, S19–S24. 10.1038/ijosup.2012.17. [PubMed: 27152149]
43. Thaler JP, Yi C-X, Schur EA, Guyenet SJ, Hwang BH, Dietrich MO, Zhao X, Sarruf DA, Izgur V, Maravilla KR, et al. (2012). Obesity is associated with hypothalamic injury in rodents and humans. *J. Clin. Investig.* 122, 153–162. 10.1172/JCI59660. [PubMed: 22201683]
44. Valdearcos M, Robblee MM, Benjamin DI, Nomura DK, Xu AW, and Koliwad SK (2014). Microglia dictate the impact of saturated fat consumption on hypothalamic inflammation and neuronal function. *Cell Rep.* 9, 2124–2138. 10.1016/j.celrep.2014.11.018. [PubMed: 25497089]

45. Weisberg SP, McCann D, Desai M, Rosenbaum M, Leibel RL, and Ferrante AW (2003). Obesity is associated with macrophage accumulation in adipose tissue. *J. Clin. Investig.* 112, 1796–1808. 10.1172/JCI19246. [PubMed: 14679176]
46. Liang W, Qi Y, Yi H, Mao C, Meng Q, Wang H, and Zheng C (2022). The roles of adipose tissue macrophages in human disease. *Front. Immunol.* 13, 908749. 10.3389/fimmu.2022.908749. [PubMed: 35757707]
47. Fujita Y, Nakanishi T, Ueno M, Itohara S, and Yamashita T (2020). Netrin-G1 Regulates Microglial Accumulation along Axons and Supports the Survival of Layer V Neurons in the Postnatal Mouse Brain. *Cell Rep.* 31, 107580. 10.1016/j.celrep.2020.107580. [PubMed: 32348754]
48. Ozdinler PH, and Macklis JD (2006). IGF-I specifically enhances axon outgrowth of corticospinal motor neurons. *Nat. Neurosci.* 9, 1371–1381. 10.1038/nn1789. [PubMed: 17057708]
49. Sakai J (2020). Core Concept: How synaptic pruning shapes neural wiring during development and, possibly, in disease. *Proc. Natl. Acad. Sci. USA* 117, 16096–16099. 10.1073/pnas.2010281117. [PubMed: 32581125]
50. Scott-Hewitt N, Perrucci F, Morini R, Erreni M, Mahoney M, Witkowska A, Carey A, Faggiani E, Schuetz LT, Mason S, et al. (2020). Local externalization of phosphatidylserine mediates developmental synaptic pruning by microglia. *EMBO J.* 39, e105380. 10.15252/embj.2020105380. [PubMed: 32657463]
51. Lehrman EK, Wilton DK, Litvina EY, Welsh CA, Chang ST, Frouin A, Walker AJ, Heller MD, Umemori H, Chen C, and Stevens B (2018). CD47 Protects Synapses from Excess Microglia-Mediated Pruning during Development. *Neuron* 100, 120–134.e6. 10.1016/j.neuron.2018.09.017. [PubMed: 30308165]
52. De Luca SN, Ziko I, Dhuna K, Sominsky L, Tolcos M, Stokes L, and Spencer SJ (2017). Neonatal overfeeding by small-litter rearing sensitises hippocampal microglial responses to immune challenge: Reversal with neonatal repeated injections of saline or minocycline. *J. Neuroendocrinol.* 29, e12540. 10.1111/jne.12540.
53. Bilbo SD, and Tsang V (2010). Enduring consequences of maternal obesity for brain inflammation and behavior of offspring. *FASEB J.* 24, 2104–2115. 10.1096/fj.09-144014. [PubMed: 20124437]
54. Crapser JD, Spangenberg EE, Barahona RA, Arreola MA, Hohsfield LA, and Green KN (2020). Microglia facilitate loss of perineuronal nets in the Alzheimer's disease brain. *EBioMedicine* 58, 102919. 10.1016/j.ebiom.2020.102919. [PubMed: 32745992]
55. Crapser JD, Ochaba J, Soni N, Reidling JC, Thompson LM, and Green KN (2020). Microglial depletion prevents extracellular matrix changes and striatal volume reduction in a model of Huntington's disease. *Brain* 143, 266–288. 10.1093/brain/awz363. [PubMed: 31848580]
56. Liu Y-J, Spangenberg EE, Tang B, Holmes TC, Green KN, and Xu X (2021). Microglia elimination increases neural circuit connectivity and activity in adult mouse cortex. *J. Neurosci.* 41, 1274–1287. 10.1523/JNEUROSCI.2140-20.2020. [PubMed: 33380470]
57. Alonge KM, Mirzadeh Z, Scarlett JM, Logsdon AF, Brown JM, Cabrales E, Chan CK, Kaiyala KJ, Bentsen MA, Banks WA, et al. (2020). Hypothalamic perineuronal net assembly is required for sustained diabetes remission induced by fibroblast growth factor 1 in rats. *Nat. Metab.* 2, 1025–1033. 10.1038/s42255-020-00275-6. [PubMed: 32895577]
58. Beddows CA, Shi F, Horton AL, Dalal S, Zhang P, Ling C-C, Yong VW, Loh K, Cho E, Karagiannis C, et al. (2024). Pathogenic hypothalamic extracellular matrix promotes metabolic disease. *Nature* 633, 914–922. 10.1038/s41586-024-07922-y. [PubMed: 39294371]
59. Chen W, Mehlkop O, Scharn A, Nolte H, Klemm P, Henschke S, Steuernagel L, Sotelo-Hitschfeld T, Kaya E, Wunderlich CM, et al. (2023). Nutrient-sensing AgRP neurons relay control of liver autophagy during energy deprivation. *Cell Metab.* 35, 786–806.e13. 10.1016/j.cmet.2023.03.019. [PubMed: 37075752]
60. Dearden L, Bouret SG, and Ozanne SE (2018). Sex and gender differences in developmental programming of metabolism. *Mol. Metabol.* 15, 8–19. 10.1016/j.molmet.2018.04.007.
61. Dearden L, and Balthasar N (2014). Sexual dimorphism in offspring glucose-sensitive hypothalamic gene expression and physiological responses to maternal high-fat diet feeding. *Endocrinology* 155, 2144–2154. 10.1210/en.2014-1131. [PubMed: 24684305]

62. Lenz KM, and McCarthy MM (2015). A starring role for microglia in brain sex differences. *Neuroscientist* 21, 306–321. 10.1177/1073858414536468. [PubMed: 24871624]
63. Schwarz JM, Sholar PW, and Bilbo SD (2012). Sex differences in microglial colonization of the developing rat brain. *J. Neurochem.* 120, 948–963. 10.1111/j.1471-4159.2011.07630.x. [PubMed: 22182318]
64. Nelson LH, Warden S, and Lenz KM (2017). Sex differences in microglial phagocytosis in the neonatal hippocampus. *Brain Behav. Immun.* 64, 11–22. 10.1016/j.bbi.2017.03.010. [PubMed: 28341582]
65. Lenz KM, Nugent BM, Haliyur R, and McCarthy MM (2013). Microglia are essential to masculinization of brain and behavior. *J. Neurosci.* 33, 2761–2772. 10.1523/JNEUROSCI.1268-12.2013. [PubMed: 23407936]
66. VanRyzin JW, Yu SJ, Perez-Pouchoulen M, and McCarthy MM (2016). Temporary Depletion of Microglia during the Early Postnatal Period Induces Lasting Sex-Dependent and Sex-Independent Effects on Behavior in Rats. *eNeuro* 3, e0297–16. 10.1523/ENEURO.0297-16.2016.
67. Valdearcos M, McGrath ER, Mayfield SB, Folick A, Cheang RT, Li L, Bachor TP, Lippert RN, Xu AW, and Koliwad SK (2022). Microglia mediate the early-life programming of adult glucose control. Preprint at biorxiv.
68. Cyphert HA, Walker EM, Hang Y, Dhawan S, Haliyur R, Bonatakis L, Avrahami D, Brissova M, Kaestner KH, Bhushan A, et al. (2019). Examining How the MAFB Transcription Factor Affects Islet β -Cell Function Postnatally. *Diabetes* 68, 337–348. 10.2337/db18-0903. [PubMed: 30425060]

Highlights

- Microglia transiently accumulate in the mediobasal hypothalamus (MBH) during neonatal life
- Microglia consume synapses and perineuronal net components in the MBH during this period
- Depleting microglia in this period reduces MBH synaptic connections to pancreatic β cells
- This reduced connectivity is linked to impaired adult insulin-dependent glucose tolerance

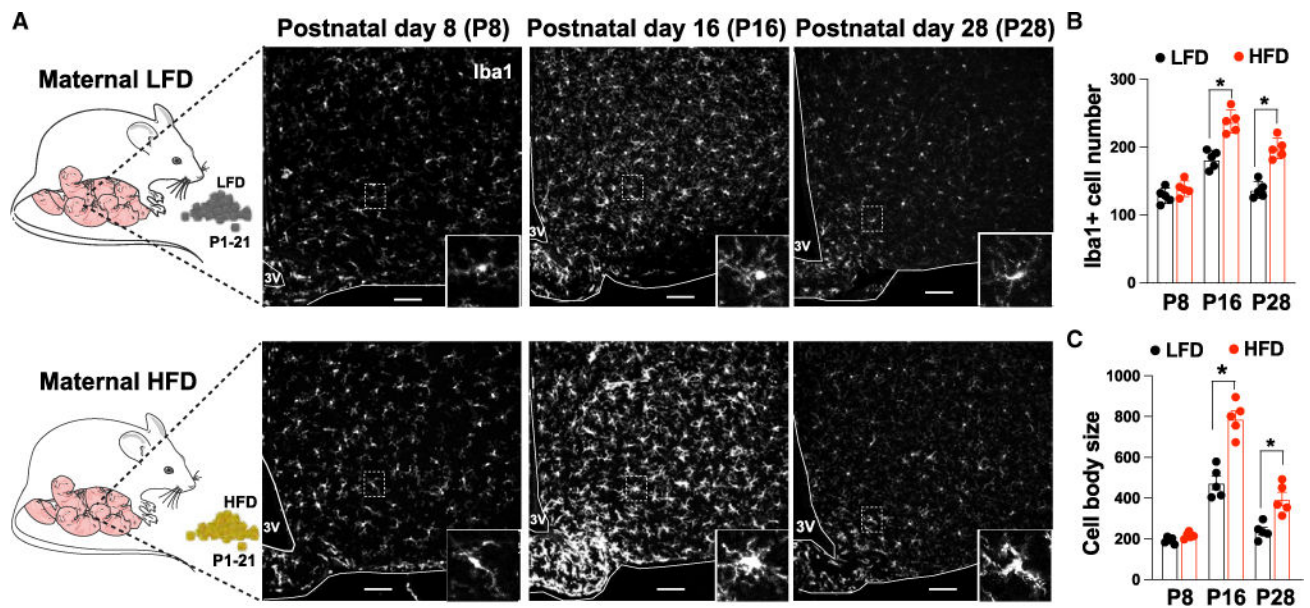


Figure 1. Microglial reactivity is transiently induced in the MBH during early postnatal life, a process potentiated by maternal consumption of an HFD

(A) Representative confocal images showing increases in the number and cell body size of Iba1⁺ microglia in the early postnatal MBH from P8 to P16, with a robust potentiation noted when comparing sections from mice nursed by dams fed an HFD (bottom) vs. the LFD (top) during lactation. In each case, substantial regression is seen at P28, 1 week after the mice were weaned onto the LFD.

(B) Quantification of microglial number in (A).

(C) Quantification of microglial cell body size in (A).

$n = 5-6/\text{group}$ (* $p < 0.05$ HFD vs. LFD). Values are mean \pm SEM (3V, third ventricle; scale bar, 20 μm).

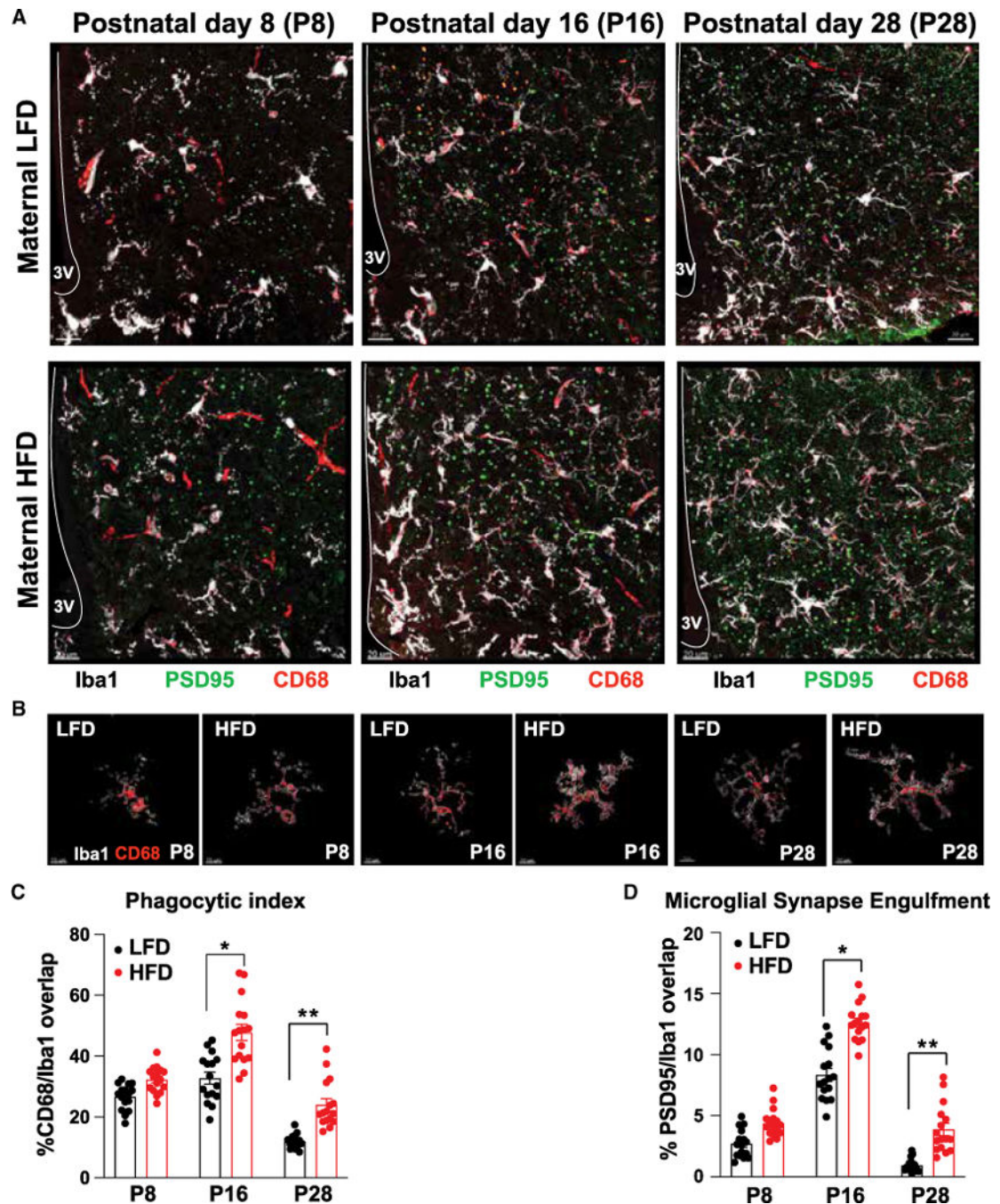


Figure 2. Microglia engage in maternal diet-responsive synaptic engulfment during early postnatal hypothalamic development

(A) Representative confocal images of MBH sections from early postnatal mice nursed by dams fed either the LFD or HFD during the lactation period, showing Iba1⁺ microglia (white), PSD-95 (postsynaptic density protein 95; green), and CD68 (red, lysosomal content).

(B) Imaris 3D surface reconstructions of representative microglia from images in (A) showing lysosomal content (CD68, red) within Iba1⁺ microglia (white) at P8, P16, and P28 in the context of either maternal LFD or HFD as in (A).

(C) Quantification of the microglial phagocytic index marked by CD68/Iba1 overlap in (B).
(D) Quantification of microglial synapse engulfment, marked by PSD-95/Iba1 overlap.
For both (C) and (D), $n = 3$ mice/condition and $n = 6$ cells/section, for a total of 48 cells analyzed per condition. All values are mean \pm SEM ($*p < 0.05$; 3V, third ventricle; scale bar, 20 μm).

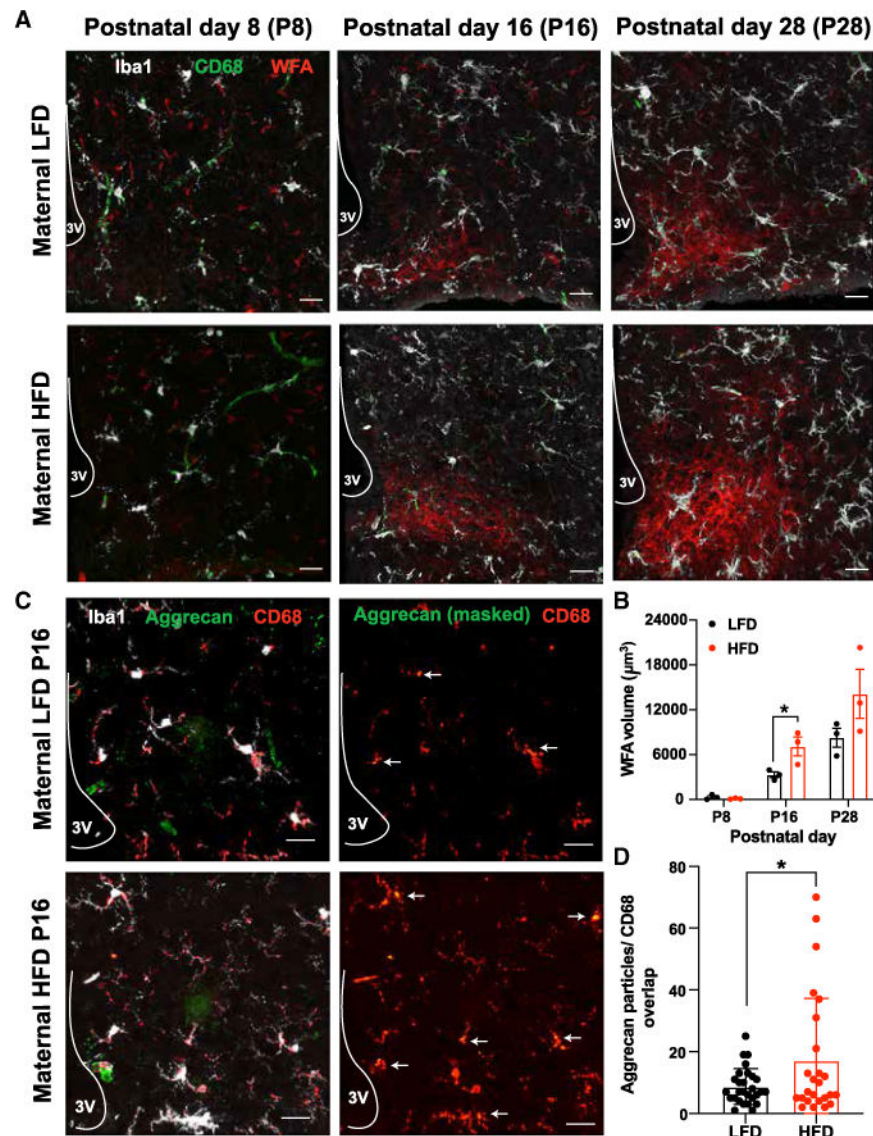


Figure 3. Microglia engulf PNNs forming within the MBH during early postnatal life, with enhancement by maternal HFD consumption

(A) Representative confocal images of MBH sections from mice at P8 and P16, respectively, nursed dams fed either the LFD or HFD during the lactation period or following weaning (P28), showing Iba1⁺ microglia (white), CD68 (green, lysosomal content), and WFA (wisteria floribunda agglutinin; red, WFA to label PNNs).

(B) Quantification of (A).

(C) Representative confocal images of P16 postnatal MBH sections under each maternal dietary condition co-stained for either the combination of Iba1⁺ (white), aggrecan (green), and CD68 (red) at left or masked aggrecan (green) to mark the chondroitin sulfate proteoglycan of PNNs within CD68 (red) content at right.

(D) Index of microglial PNN engulfment assessed by quantifying the overlap aggrecan and CD68 (lysosomal content) based on Imaris 3D surface reconstructions of representative microglia from sections stained as in (B).

For (B), $n = 3$ mice per group, $n = 5$ –6 sections/mice. For (D), $n = 5$ mice per group, 3 MBH sections per mouse, and a total of 26–28 images analyzed per condition. Each dot in (C) represents the number of discrete aggrecan particles within a CD68⁺ volumetric region across each section analyzed. All values are mean \pm SEM ($*p < 0.05$; 3V, third ventricle; scale bar, 20 μm).

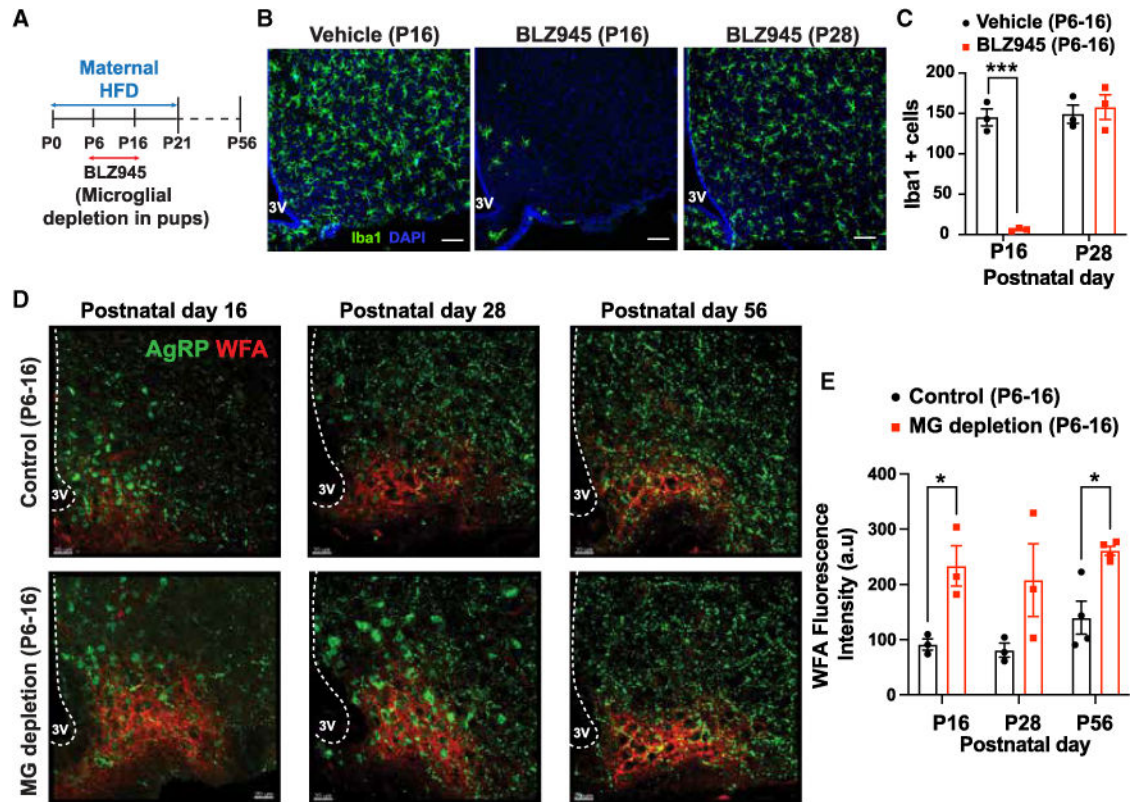


Figure 4. Depleting microglia specifically during early postnatal life durably increases PNN abundance within the MBH

(A) Experimental design to assess the impact of postnatal microglial depletion from P6 to P16 using BLZ945 treatment (200 mg/kg, every other day, i.p.) while dams are fed an HFD during lactation.

(B) Representative confocal images of MBH sections showing Iba1+ (green) microglia repopulation after drug withdrawal (P16).

(C) Quantification of (B) (***) $p < 0.001$.

(D) Representative confocal images showing cell bodies and axonal projections of AgRP (green) neurons and WFA (wisteria floribunda agglutinin; red, WFA to label perineuronal nets) at P16, P28, and P56.

(E) Quantification of WFA fluorescence intensity in (D) (* $p < 0.05$; $n = 3$ mice/condition).

All values are mean \pm SEM (3V, third ventricle; scale bar, 20 μ m).

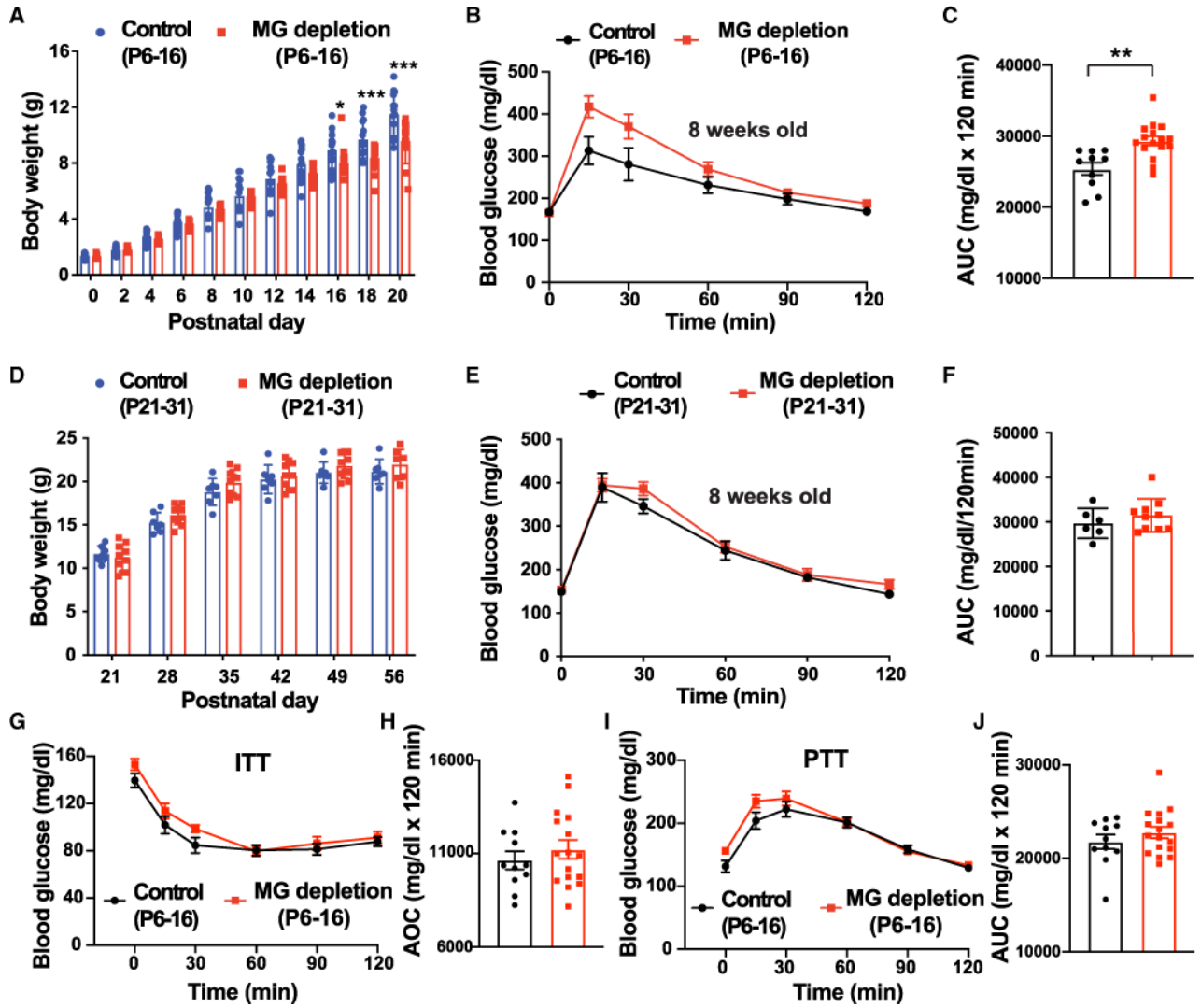


Figure 5. Early postnatal microglial depletion is sufficient to induce glucose intolerance in adulthood

(A) Depleting microglia using systemic BLZ945 treatment from P6 to P16 in the context of maternal HFD consumption during the lactating period led to a reduction in the rate of body weight gain among the pups during the period prior to weaning as compared to control pups.

* $p < 0.05$ and *** $p < 0.001$ ($n = 10-16$ /group).

(B) Microglial depletion as in (A) was associated with a worsening of glucose tolerance as assessed by GTT at P56 ($n = 10-16$ /group).

(C) Quantification of data in (B) using area under the curve (AUC) analysis (** $p < 0.01$).

(D and E) Equivalent body weights (D) and glucose tolerance (E) in mice at P56 when microglia were depleted from P21 to P31 after weaning had occurred.

(F) AUC of data in (E).

(D-F) $n = 6-10$ /group.

(G) Similar insulin tolerance (ITT) at 9 weeks of age in mice having undergone microglial depletion from P6 to P16 as in (A) vs. control.

(H) Quantification of data in (G) by AUC analysis ($n = 11-16$ /group).

(I) Equivalent pyruvate tolerance (PTT) at 10 weeks of age in mice having undergone microglial depletion from P6 to P16 as in (A) vs. control.
(J) Quantification of data in (I) by AUC analysis ($n = 11-16$).
All values are mean \pm SEM.

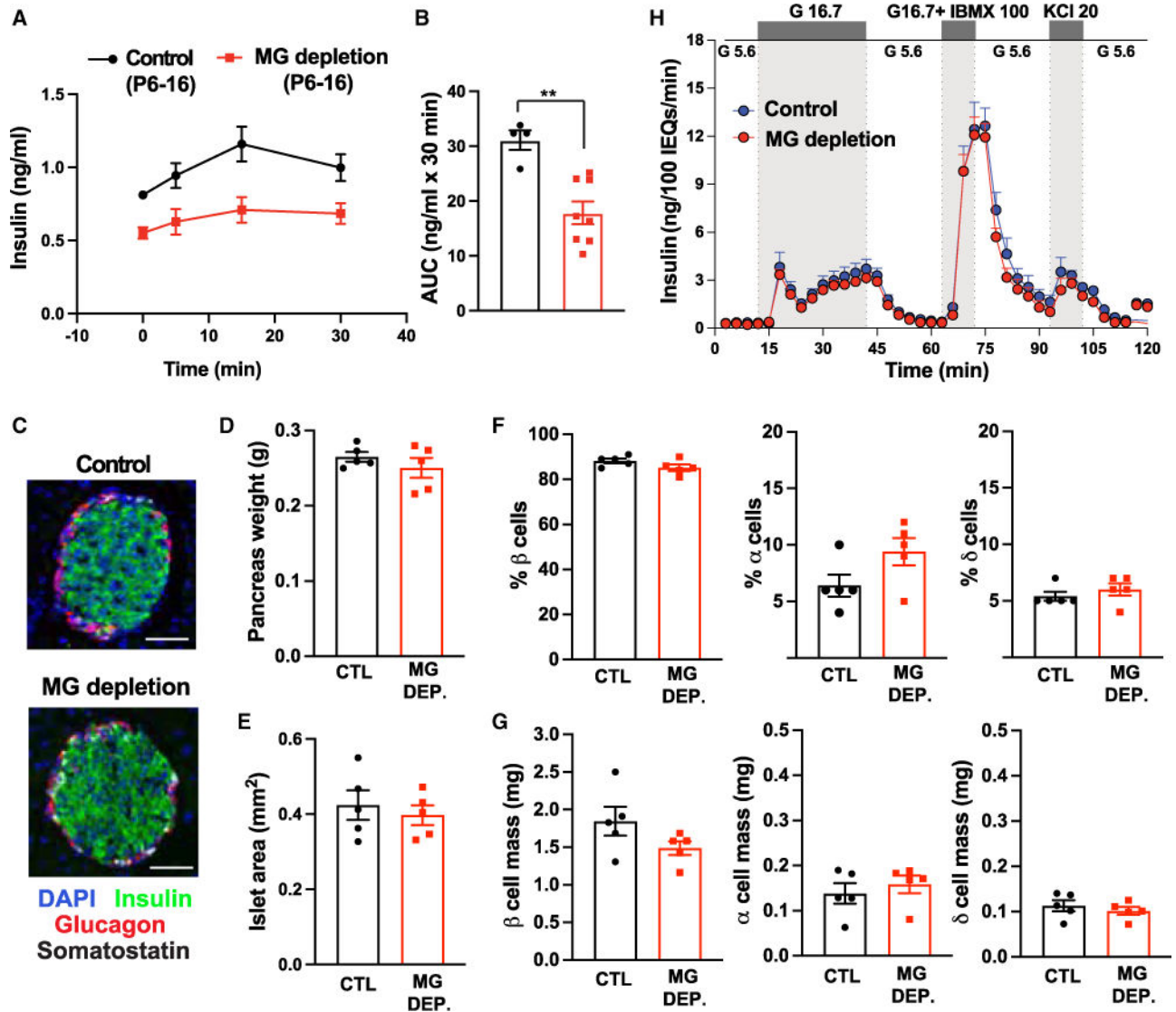


Figure 6. Depleting microglia specifically during early postnatal life is sufficient to impair the insulinemic response to a glucose challenge in adulthood without impacting islet mass or maturation

(A) Reduced plasma insulin levels, both under fasting conditions and in the context of an i.p. GTT (2 g glucose/kg), in 8-week-old mice that underwent microglial depletion from P6 to P16 vs. control littermates.

(B) AUC quantification of data in (A) ($n = 4-8/\text{group}$). $**p < 0.01$.

(C) Representative images of islets from the pancreata of 8-week-old mice that underwent microglial depletion from P6 to P16 vs. control littermates showing DAPI (blue), insulin (green), glucagon (red), and somatostatin (white).

(D–H) Equivalent pancreas weights (D), islet areas (E), islet cellular composition (based on data in C) (F), specific cellular masses within the islets (G), and levels of glucose-stimulated insulin secretion by isolated islets (H) in 8-week-old mice that underwent microglial depletion from P6 to P16 vs. control littermates ($n = 4-8/\text{group}$).

All values are mean \pm SEM. Scale bar, 50 μm .

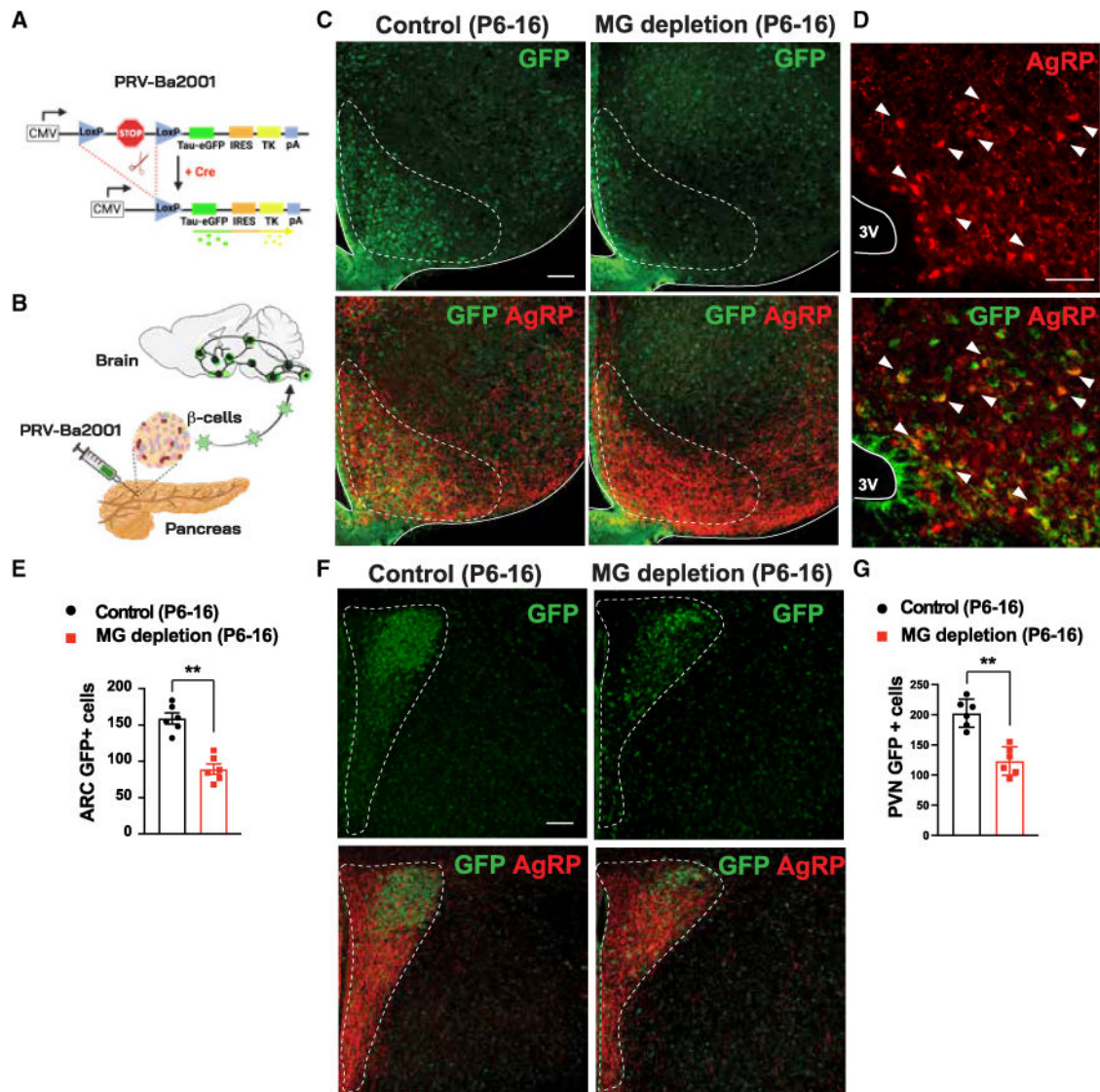


Figure 7. Microglia are required during early postnatal life to ensure normal synaptic connectivity between hypothalamic neurons and β cells

(A) Structure and expression properties of pseudorabies virus (PRV) strain Ba2001 that is dependent on Cre-mediated recombination for the expression of GFP and thymidine kinase (TK), a viral protein that promotes efficient replication.

(B) Schematic of the protocol for Ba2001 delivery into the pancreas of MIP-Cre^{ER} mice in order to label neurons specifically innervating insulin-expressing β cells and trace these efferent neurons using GFP expression in retrograde fashion across multiple synapses into the brain.

(C) Representative images of MBH sections from 8-week-old mice treated as in (B) showing GFP⁺ neurons (green) in the ARC that are synaptically connected to pancreatic β cells and the dramatic reduction in these labeled neurons, including those co-labeled with AgRP, within the ARC of mice that underwent transient microglial depletion from P6 to P16.

(D) Higher-resolution images of sections in (C) more clearly revealing the co-localization between GFP and AgRP cell bodies (red).

(E) Quantification of data from images as in (D) showing the reduction in GFP⁺ neurons within the ARC of mice that underwent transient microglial depletion from P6 to P16 ($n = 6/\text{group}$, $**p < 0.01$).

(F) Representative images, analogous to those in (C), showing impact of early-life microglial depletion on sharply reducing the number of GFP⁺ neurons (green) within PVH that are synaptically connected to the β cell compartment at 8 weeks of life.

(G) Quantification of data in (F) ($n = 6/\text{group}$, $**p < 0.01$).

All values are mean \pm SEM (3V, third ventricle; scale bar, 20 μm).

KEY RESOURCES TABLE

REAGENT or RESOURCE	SOURCE	IDENTIFIER
Antibodies		
Rabbit polyclonal anti- Iba1	FUJIFILM Wako Pure Chemical Corporation	Cat# 019-19741; RRID:AB_839504
Goat polyclonal anti-Iba1	Abcam	Cat# ab107159; RRID:AB_10972670
Rat Anti-Mouse CD68 Monoclonal Antibody	Bio-Rad	Cat# MCA1957; RRID:AB_322219
Rabbit polyclonal anti-PSD95	Synaptic Systems	Cat# 124 003; RRID:AB_2725761
Rabbit polyclonal anti-AggreCAN	Millipore	Cat# AB1031; RRID:AB_90460
Goat polyclonal anti- AgRP	Neuromics	Cat# GT15040; RRID:AB_2737180
Chicken polyclonal anti-GFP	Aves Labs	Cat# GFP-1010; RRID:AB_2307313
Guinea pig polyclonal anti-insulin	Fitzgerald Industries International	Cat# 20-IP35; RRID:AB_231771
Rabbit polyclonal anti-glucagon	Cell Signaling Technology	Cat# 8233; RRID:AB_10859908
Bacterial and virus strains		
PRV-Ba2001	PNI (Princeton Neuroscience Institute) Viral Vector Core Facility	N/A
Chemicals, peptides, and recombinant proteins		
Tamoxifen, Free Base	MP Biomedicals	Cat# 156738
PLX5622	Plexxikon	N/A
BLZ945	APExBIO	Cat# B4899
Captisol 20%	Cydx Pharmaceuticals	RC0C7100
Wisteria Floribunda Lectin (WFA, WFL), Biotinylated	Vector Laboratories	B-1355-2
Critical commercial assays		
Mouse Insulin ELISA	Crystal Chem	Cat#90080
Experimental models: Organisms/strains		
B6.Cg-Tg(Ins1-cre/ERT)1Lphi/J	The Jackson Laboratory	JAX:024709
Software and algorithms		
Imaris 9.5.1	Oxford Instruments	N/A
GraphPad Prism 8.0	GraphPad	N/A